ISSN 0031-918X, Physics of Metals and Metallography, 2019, Vol. 120, No. 3, pp. 290–295. © Pleiades Publishing, Ltd., 2019.
Russian Text © N.N. Popov, T.I. Sysoeva, D.V. Presnyakov, A.A. Kostyleva, 2019, published in Fizika Metallov i Metallovedenie, 2019, Vol. 120, No. 3, pp. 313–319.

STRENGTH AND PLASTICITY

# Effect of the Rate, Temperature, and Magnitude of Prestraining on the Parameters of Phase Transformations and the Thermomechanical Characteristics of the 45% Ti–45% Ni–10% Nb Shape Memory Alloy in Press-Formed Conditions

**N. N. Popov[a], *, T. I. Sysoeva[a], D. V. Presnyakov[a], and A. A. Kostyleva[a]**

[a]*Russian Federal Nuclear Center All-Russia Research Institute of Experimental Physics, Sarov, Nizhny Novgorod oblast, 607188 Russia*

**e-mail: popov@astra.vniief.ru*

Received April 9, 2018; revised September 4, 2018; accepted September 21, 2018

**Abstract**—This work investigates the effect of the rate, temperature, and magnitude of the strain induced preliminarily to heating for developing shape memory effect on the phase composition, martensite transformation, phase transition temperature, lattice parameters, substructure parameters, and thermomechanic characteristics of the shape memory (SM) 45Ti–45Ni–10Nb (at %) alloy in the press-formed state. The relation between structural and thermomechanical parameters of the alloy is identified. The conditions of prestraining the SM alloy for achieving the best thermomechanic characteristics are determined. The results of this study have been used to develop a fire-protection device for nuclear power facilities.

*Keywords:* 45Ti–45Ni–10Nb (at %) alloy, shape memory effect (SME), press-formed state (condition), conditions of prestraining, phase composition, kinetics of phase transition, phase transition temperature, lattice parameters, substructural parameters, thermomechanic properties

**DOI:** 10.1134/S0031918X19030104

## INTRODUCTION

Shape memory alloys (SMAs) of the Ti–Ni–Fe system have usually been used for the thermomechanical connection of pipelines [1, 2]. However, couplings made of these alloys must be mandrel-pressed, stored, and installed at cryogenic temperatures. Russian researchers have therefore suggested using additional alloying of titanium nickelide with niobium to expand the martensitic hysteresis of SMAs [3–5]. A great number of papers on this topic are given in [6]. We investigated Ti–Ni–Nb SMAs in the cast state, and, later, in the pressed-formed condition [7–10]. The effect of a number of factors on the properties of Ti–Ni–Nb SMAs was studied in detail in [5, 6, 11, 12]. However, a comprehensive study of the effect of various prestraining conditions on the shape memory effect (SME) in the 45Ti–45Ni–10Nb (at %) alloy was not performed. Therefore, the aim of this work is to study the effect of the temperature and rate of applying preliminary straining on the phase transformation parameters and thermomechanical characteristics of the 45Ti–45Ni–10Nb (at %) alloy in the press-formed state.

## EXPERIMENTAL

We studied the 45Ti–45Ni–10Nb (at %) SMA of batch no. 193-11-p delivered as a pressed rod 25 mm in diameter. Samples and the metallographic polished section to be investigated were prepared. Samples for X-ray structural studies are described in [9], and for the study of thermomechanical characteristics, in [7]. We annealed the samples under the following conditions: heating in a vacuum furnace to a temperature of 850°C, holding for 4 h, and furnace cooling. The samples were then subjected to tensile tests (for prestraining) under various temperature, rate, and deformation conditions.

The phase composition, crystal lattice and substructural parameters, and characteristics of martensitic transformations (MTs) in the alloy samples in the initial state and after annealing were determined using an X-ray diffractometer in Cu $K\alpha$ radiation at a power of 18 kW, as described in [3]. Tensile tests of the samples were carried out on a UTS-100K testing machine to find the thermomechanical characteristics of the alloy and to build stress–strain ($\sigma$–$\varepsilon$) diagrams. After deformation, the investigated samples were placed into a thermochamber of an R1084 unit to heat the samples to a temperature of $T = 100$°C at a heating rate of 4 K/min. Then, the samples were cooled to $T = -170$°C. Heating made them shorter and resulted in the shape memory effect. Upon cooling, no reversible shape memory effect was observed. The shape recovery diagrams of the alloy samples were used to deter-

mine characteristic temperatures $A^{b}_{s\,SME}$ and $A^{e}_{f\,SME}$ at the beginning and at the end of the entire shape recovery range, respectively, where SME manifests itself. The tangential method was used to find characteristic temperatures $A_{s\,SME}$ and $A_{f\,SME}$, which characterize the main shape recovery in the $A^{b}_{s\,SME}-A^{e}_{f\,SME}$ temperature range. The degree of shape recovery $\eta_{SME}$ during SME was found from

$$\eta_{SME} = \frac{\varepsilon_{SME}}{\varepsilon_r},$$

where $\varepsilon_{SME}$ is the thermally reversible deformation during SME and $\varepsilon_r$ is the residual deformation after unloading [14].

## RESULTS AND DISCUSSION

**1. MT in the course of development of SME during heating in the 45Ti–45Ni–10Nb alloy after its preliminary deformation by tension.** The X-ray diffraction (XRD) analysis was used to investigate reverse MT in the alloy samples during heating-induced SME after preliminary deformation by tension under various conditions (varying the strain $\varepsilon_0$ preliminary to SME-initiating holding at constant temperature $T_d$ and deformation rate $\dot{\varepsilon}$, or changing $T_d$ at fixed $\varepsilon_0$ and $\dot{\varepsilon}$, or changing $\dot{\varepsilon}$ at fixed $\varepsilon_0$ and $T_d$).

Figure 1 shows an example of XRD patterns taken at different total prestraining deformations $\varepsilon_0 = 6\%$ and $\varepsilon_0 = 30\%$. The study allowed us to build martensitic curves to determine the temperatures of the reverse MT ($A'_{s\,SME}$, $A'_{f\,SME}$ are the temperatures of the start and finish of the reverse MT during SME). The measurement error was ±5 K.

Table 1 suggests that 100% *B*19' martensite is formed upon deformation of the alloy from 6 to 30% by tension at –60...–70°C. Subsequent heating in the temperature range from –60°C to 100°C results in the SME and the reverse MT of the TiNi phase. The MT in samples deformed to 6, 11, and 15% occurs completely and it develops according to the scheme *B*19' → *B*2. In samples deformed to 30%, the transformation is incomplete and it develops according to the scheme *B*19'→ (*B*2 + *B*19'). The remarkable thing is that heating in this case was carried out only up to a temperature of 100°C, because of the limited capabilities of the equipment employed.

Martensite *B*19' is also formed upon the deformation of the alloy samples by tension at different temperatures (at a constant prestraining deformation equal to 11% and the deformation rate equal to $1.2 \times 10^{-3}$ $s^{-1}$). As the deformation temperature increases from –60...–70 to 24°C, the amount of the martensite decreases. The fraction of the martensite formed upon deformation at 24°C is 55%.

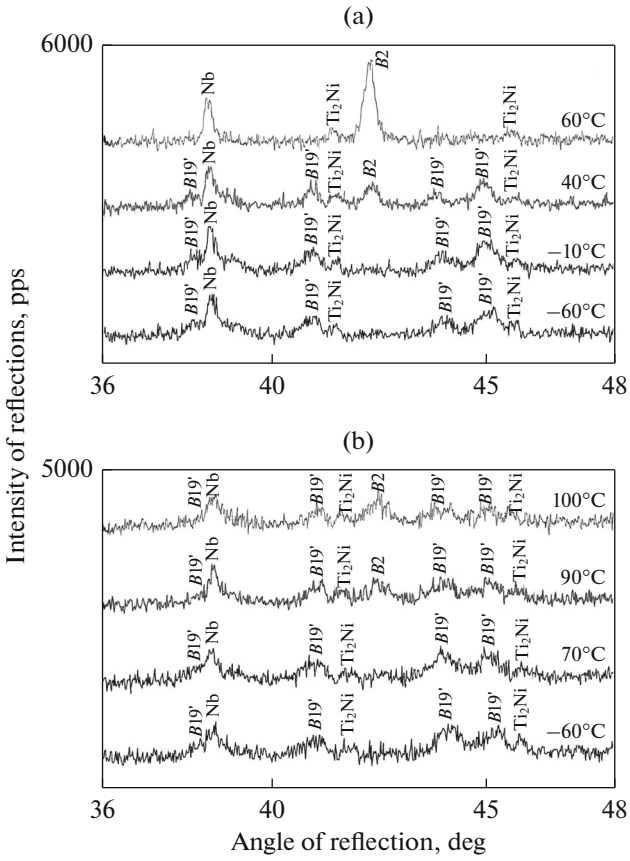


**Fig. 1.** X-ray diffraction patterns taken at different temperatures for the press-formed 45Ti–45Ni–10Nb alloy after tension $\varepsilon_0$ = (a) 6 and (b) 30% (at $T_d$ = –60...–70°C, $\dot{\varepsilon} \approx 1.2 \times 10^{-3}$ $s^{-1}$).

Subsequent heating from –60°C to 100°C causes complete MT according to the scheme *B*19' → *B*2 in the samples deformed at –60...–70 and 0...–5°C. The transformation in the samples deformed at a temperature of 24°C develops according to the scheme (*B*19' + *B*2) → (*B*2 + *B*19') and it is not completed.

The deformation of the samples by tension at different deformation rates and a constant prestraining deformation that is 11% and a temperature of –60...–70°C causes the formation of 100% *B*19' martensite. Its amount remains the same even after the deformation rate is increased from $1.2 \times 10^{-3}$ to $1.2 \times 10^{-1}$ $s^{-1}$. The reverse *B*19' → *B*2 MT is observed in all the samples upon heating from –60°C to 100°C.

Table 1 suggests that the temperatures of the reverse MT increase when the value of the prestraining deformation $\varepsilon_0$ increases from 6 to 30%.

No effect of the deformation temperature in the range from –60...–70 to 0...–5°C on the temperature of the reverse MT was observed. The temperature range of the reverse MT $|A'_{s\,SME} - A'_{f\,SME}|$ expands when the second deformation temperature range is

**Table 1.** Schemes and the temperatures of the onset and finish of the reverse MT in the annealed samples of the press-formed 45Ti–45Ni–10Nb (at %) alloy during SME after tension (preceding the heating that initiates SME) performed under various conditions

| Deformation conditions | Scheme of MT upon heating and the percentage content of *B*2 austenite and *B*19' martensite | Temperatures of the start and finish of the reverse MT during SME, °C | | Width of the range $\lvert A'_{s\ SME} - A'_{f\ SME}\rvert$, K |
|---|---|---|---|---|
| | | $A'_{s\ SME}$ | $A'_{f\ SME}$ | |
| $T_d = -60...-70$°C, $\dot{\varepsilon} \approx 1.2 \times 10^{-3}$ s$^{-1}$ | | | | |
| $\varepsilon_0 = 6\%$ | 100% *B*19' → 100% *B*2 | 30 | 50 | 20 |
| $\varepsilon_0 = 11\%$ | 100% *B*19' → 100% *B*2 | 50 | 70 | 20 |
| $\varepsilon_0 = 15\%$ | 100% *B*19' → 100% *B*2 | 65 | 80 | 15 |
| $\varepsilon_0 = 30\%$ | 100% *B*19' → 50% *B*2 + 50% *B*19' | 90 | >100 | >10 |
| $\varepsilon_0 = 11\%$, $\dot{\varepsilon} \approx 1.2 \times 10^{-3}$ s$^{-1}$ | | | | |
| $T_d = -60...-70$°C | 100% *B*19' → 100% *B*2 | 50 | 70 | 20 |
| $T_d = 0...-5$°C | 100% *B*19' → 100% *B*2 | 50 | 70 | 20 |
| $T_d = 24$°C | 55% *B*19' + 45% *B*2 → 70% *B*2 + 30% *B*19' | 60 | >100 | >40 |
| $\varepsilon_0 = 11\%$, $T_d = -60...-70$°C | | | | |
| $\dot{\varepsilon} \approx 1.2 \times 10^{-3}$ s$^{-1}$ | 100% *B*19' → 100% *B*2 | 50 | 70 | 20 |
| $\dot{\varepsilon} \approx 1.2 \times 10^{-2}$ s$^{-1}$ | 100% *B*19' → 100% *B*2 | 55 | 70 | 15 |
| $\dot{\varepsilon} \approx 1.2 \times 10^{-1}$ s$^{-1}$ | 100% *B*19' → 100% *B*2 | 50 | 70 | 20 |

**Table 2.** Phase composition at 30°C in the annealed samples of the press-formed 45Ti–45Ni–10Nb alloy after SME induced by prestraining tension under various conditions

| Deformation conditions | | TiNi (*B*2), % | TiNi (*B*19'), % | Nb, % | $Ti_2Ni$, % |
|---|---|---|---|---|---|
| $T_d = -60...-70$°C, $\dot{\varepsilon} \approx 1.2 \times 10^{-3}$ s$^{-1}$ | $\varepsilon_0 = 6\%$ | 60.1 | 0 | 34.3 | 5.6 |
| | $\varepsilon_0 = 11\%$ | 53.0 | 4.2 | 37.2 | 5.6 |
| | $\varepsilon_0 = 15\%$ | 48.6 | 9.3 | 36.2 | 5.9 |
| | $\varepsilon_0 = 30\%$ | 20.2 | 39.7 | 34.3 | 5.8 |
| $\varepsilon_0 = 11\%$, $\dot{\varepsilon} \approx 1.2 \times 10^{-3}$ s$^{-1}$ | $T_d = -60...-70$°C | 59.3 | 4.4 | 30.7 | 5.6 |
| | $T_d = 0...-5$ °C | 62.0 | 4.2 | 32.4 | 5.2 |
| | $T_d = 24$°C | 46.8 | 13.5 | 33.7 | 6.0 |
| $\varepsilon_0 = 11\%$, $T_d = -60...-70$°C | $\dot{\varepsilon} \approx 1.2 \times 10^{-1}$ s$^{-1}$ | 51.2 | 4.2 | 37.2 | 7.4 |
| | $\dot{\varepsilon} \approx 1.2 \times 10^{-2}$ s$^{-1}$ | 58.0 | 1.7 | 33.5 | 6.8 |
| | $\dot{\varepsilon} \approx 1.2 \times 10^{-1}$ s$^{-1}$ | 55.3 | 2.5 | 34.9 | 7.3 |

from 0...–5 to 24°C. In this case, the temperatures of the reverse MT during SME significantly increase. Here, the shift of temperature $A'_{f\ SME}$ is pronounced. This is the result of high-temperature SME associated with the stabilization of plastically deformed martensite [15].

Analysis of the effect of the prestraining deformation rate on the temperatures of the reverse MT showed that an increase in the deformation rate from $1.2 \times 10^{-3}$ to $1.2 \times 10^{-1}$ s$^{-1}$ has almost no effect on the temperatures of the reverse MT (except temperature $A'_{s\ SME}$) and their range $\lvert A'_{s\ SME} - A'_{f\ SME}\rvert$.

**2. Phase composition and the structure of the 45Ti–45Ni–10Nb alloy in the course of SME after prestraining deformation by tension performed under various conditions.** The XRD analysis of the phase composition of the alloy showed three phases (Table 2):

—the main TiNi phase is present in two states (Table 2), namely, in the form of *B*2 austenite with an ordered bcc structure and *B*19' martensite with a distorted monoclinic orthorhombic crystal lattice (except for the prestraining deformation $\varepsilon_0 = 6\%$);

—bcc Nb phase; and

—a small amount of the fcc $Ti_2Ni$ phase.

**Table 3.** TiNi (*B*2) substructural and lattice parameters of the annealed samples of the press-formed 45Ti–45Ni–10Nb alloy after SME induced by prestraining tension under various conditions

| Deformation conditions | | Lattice parameter of TiNi (*B*2), *a*, Å | Degree of microdeformation of the lattice, $\times 10^{-3}$ | Average block size, nm | Dislocation density, $cm^{-2}$ | |
|---|---|---|---|---|---|---|
| | | | | | at block boundaries, $\times 10^{11}$ | inside blocks, $\times 10^{11}$ |
| $T_d = -60...-70°C$, | $\varepsilon_0 = 6\%$ | 3.0174 | 1.9 | 25 | 5.1 | 0.3 |
| $\dot{\varepsilon} \approx 1.2 \times 10^{-3}\ s^{-1}$ | $\varepsilon_0 = 11\%$ | 3.0183 | 2.0 | 20 | 8.8 | 0.3 |
| | $\varepsilon_0 = 15\%$ | 3.0332 | 2.2 | 20 | 8.8 | 0.4 |
| | $\varepsilon_0 = 30\%$ | 3.0406 | 2.4 | 15 | 11.7 | 0.5 |
| $\varepsilon_0 = 11\%$, | $T_d = -60...-70°C$ | 3.0183 | 2.0 | 20 | 8.8 | 0.3 |
| $\dot{\varepsilon} \approx 1.2 \times 10^{-3}\ s^{-1}$ | $T_d = 0...-5°C$ | 3.0191 | 2.6 | 20 | 8.5 | 0.2 |
| | $T_d = 24°C$ | 3.0255 | 2.8 | 15 | 11.5 | 1.1 |
| $\varepsilon_0 = 11\%$, | $\dot{\varepsilon} \approx 1.2 \times 10^{-3}\ s^{-1}$ | 3.0183 | 1.9 | 20 | 7.7 | 0.3 |
| $T_d = -60...-70°C$ | $\dot{\varepsilon} \approx 1.2 \times 10^{-2}\ s^{-1}$ | 3.0151 | 1.2 | 20 | 7.5 | 0.1 |
| | $\dot{\varepsilon} \approx 1.2 \times 10^{-1}\ s^{-1}$ | 3.0154 | 1.7 | 20 | 7.5 | 0.2 |

Table 3 lists the parameters of the substructure and the TiNi (*B*2)-phase crystal lattice in the alloy.

The lattice parameter of the TiNi (*B*2) phase after prestraining deformation of the 45Ti–45Ni–10Nb alloy to $\varepsilon_0 = 15–30\%$ (at $T_d = -60...-70°C$ and $\dot{\varepsilon} \approx 1.2 \times 10^{-3}\ s^{-1}$), as well as at a prestraining deformation temperature of 24°C ($\varepsilon_0 = 11\%$, $\dot{\varepsilon} \approx 1.2 \times 10^{-3}\ s^{-1}$; see Table 3) is significantly different from that given in a handbook [16] ($a$ = 3.015 Å for a two-component Ti–Ni alloy).

This is because the TiNi phase under the above-mentioned prestraining deformation conditions exists in the intermediate two-phase (*B*2 + *B*19') state (see Table 2). The amount of the *B*19' phase is more than 5% (the error of the determination of the phase content in the alloy by the method of semiquantitative analysis is within 5%). The crystal lattice of the *B*19' phase is matched with the crystal lattice of the *B*2 phase and the atoms at the interphase boundary obey the crystalline order characteristic of both phases. This good matching between the two lattices requires a certain elastic deformation in the location of joining, which generates an elastic field of coherent stresses. Stresses change the lattice parameter [17].

The minimum number of structural defects (dislocations) characterizes the dislocation substructure of the alloys, which was formed after SME resulted from preliminary tensile deformation $\varepsilon_0$ in the range from 6 to 11% (at $T_d = -60...-70°C$, $\dot{\varepsilon} \approx 1.2 \times 10^{-3}\ s^{-1}$), at temperatures $T_d$ in the range from –60...–70°C to 0...–5°C (at $\varepsilon_0 = 11\%$, $\dot{\varepsilon} \approx 1.2 \times 10^{-3}\ s^{-1}$), and deformation rates $\dot{\varepsilon}$ from $1.2 \times 10^{-3}$ to $1.2 \times 10^{-1}\ s^{-1}$ (at $\varepsilon_0 = 11\%$, $T_d = -60...-70°C$). Correspondingly, the alloy contains fewer obstacles for MT propagation (Table 3).

The MT in this case takes place at lower temperatures and its rate is higher; that is, its range is narrower (Table 1).

**3. Thermomechanical characteristics of the 45Ti–45Ni–10Nb SMA at development of SME after prestraining deformation by tension performed under various conditions.** Figure 2 shows typical shape recovery diagrams taken during SME exhibited by the samples preliminarily deformed at different rates.

Average thermomechanical characteristics resulted from the processing of the diagrams (considering the instrumental error) are listed in Table 4.

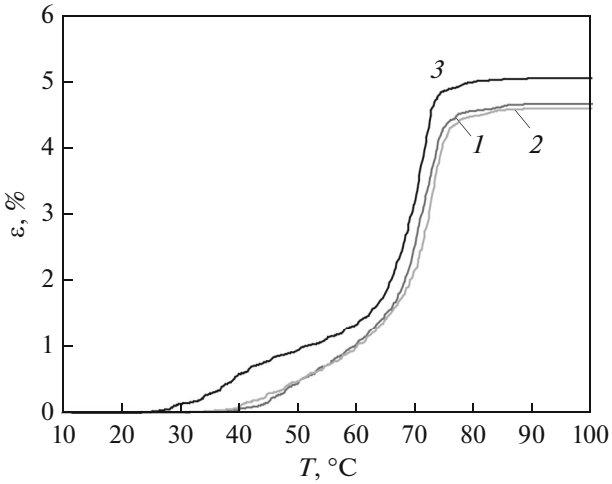


**Fig. 2.** Shape recovery curves of the 45Ti–45Ni–10Nb alloy during SME after prestraining tension by $\varepsilon_0 = 11\%$ at $T = -40...-45°C$ and different (prestraining) deformation rates $\dot{\varepsilon}$: (*1*) $1.2 \times 10^{-3}$, (*2*) $1.2 \times 10^{-2}$, and (*3*) $1.2 \times 10^{-1}\ s^{-1}$.

**Table 4.** Thermomechanical characteristics of the press-formed and annealed 45Ti–45Ni–10Nb alloy during SME after preliminary tension performed under various conditions

| Thermomechanical characteristics | Prestraining deformation conditions | | | | | | | | | |
|---|---|---|---|---|---|---|---|---|---|---|
| | $T_d = -60\ldots-70$°C, $\dot{\varepsilon} \approx 1.2 \times 10^{-3}$ s$^{-1}$ | | | | $\varepsilon_0 = 11\%$, $\dot{\varepsilon} \approx 1.2 \times 10^{-3}$ s$^{-1}$ | | | $\varepsilon_0 = 11\%$, $T_d = -40\ldots-45$°C | | |
| | $\varepsilon_0$, % | | | | $T_d$, °C | | | $\dot{\varepsilon}$, s$^{-1}$ | | |
| | 6 | 11 | 15 | 30 | –60…–70 | 0…–5 | 24 | $1.2 \times 10^{-3}$ | $1.2 \times 10^{-2}$ | $1.2 \times 10^{-1}$ |
| $\varepsilon_r$, % | 4.2 | 8.2 | 11.5 | 23.4 | 8.2 | 8.6 | 7.9 | 8.6 | 8.3 | 8.7 |
| $A^b_{s\,SME}$, °C | 34 | 23 | 42 | 20 | 23 | 15 | 42 | 32 | 32 | 24 |
| $A^e_{f\,SME}$, °C | 65 | 97 | 112 | 140 | 97 | 79 | 109 | 92 | 91 | 89 |
| $A_{s\,SME}$, °C | 55 | 65 | 74 | 67 | 65 | 51 | 52 | 64 | 66 | 63 |
| $A_{f\,SME}$, °C | 62 | 75 | 86 | 100 | 75 | 66 | 94 | 75 | 76 | 74 |
| $\varepsilon_{SME}$, % | 2 | 4.4 | 5.7 | 4.7 | 4.4 | 6.1 | 1.1 | 4.7 | 4.6 | 5.1 |
| $\eta_{SME}$ | 0.48 | 0.53 | 0.5 | 0.2 | 0.53 | 0.68 | 0.16 | 0.55 | 0.55 | 0.59 |
| $\lvert A_{s\,SME} - A_{f\,SME}\rvert$, K | 7 | 12 | 12 | 33 | 12 | 15 | 42 | 13 | 13 | 9 |

The statistical processing and the correlation analysis of the results [18–20] listed in Table 4 have revealed a significant effect of the value and temperature of the prestraining deformation preceding the initiation of SME on every thermomechanical characteristic of the alloys.

The temperatures of the beginning of shape recovery $A^b_{s\,SME} = 42$°C and $A_{s\,SME} = 74$°C, which are above room temperature, in the press-formed 45Ti–45Ni–10Nb alloy can be achieved at a preliminary (to SME) prestraining tensile deformation of $\varepsilon_0 = 15\%$ at a rate $\dot{\varepsilon} \approx 1.2 \times 10^{-3}$ s$^{-1}$ and $T_d = -60...-70$°C. The values of the SME characteristics are maximum ($\varepsilon_{SME} = 5.7\%$, $\eta_{SME} = 0.5$).

Table 4 suggests that the temperatures of the beginning of shape recovery $A^b_{s\,SME} = 42$°C and $A_{s\,SME} = 52$°C, which are above room temperature, and the range $\lvert A_{s\,SME} - A_{f\,SME}\rvert = 42$ K at the deformation temperature $T_d = 24$°C can be achieved in the alloy when temperature $T_d$ of preliminary tension (deformation rate $\dot{\varepsilon} \approx 1.2 \times 10^{-3}$ s$^{-1}$ and total deformation $\varepsilon_0 = 11\%$) is increased from –60...–70 to 24°C. However, the SME characteristics significantly decrease: $\varepsilon_{SME}$ decreases from 6.1 to 1.1% and $\eta_{SME}$, from 0.68 to 0.16. The SME characteristics ($\varepsilon_{SME} = 6.1\%$, $\eta_{SME} = 0.68$) of this alloy can be maximum at the deformation temperature $T_d = 0...-5$°C, however, the temperature of the beginning of the shape recovery is minimal ($A^b_{s\,SME} = 15$°C).

Analysis of data listed in Table 4 showed that an increase in the deformation rate from $1.2 \times 10^{-3}$ to $1.2 \times 10^{-1}$ s$^{-1}$ does not change temperatures $A^e_{f\,SME}$, $A_{s\,SME}$, and $A_{f\,SME}$, as well as $\varepsilon_{SME}$, $\eta_{SME}$, whereas it decreases $A^b_{s\,SME}$ from 32 to 24°C and $\lvert A_{s\,SME} - A_{f\,SME}\rvert$ from 13 to 9°C.

As a result, the study of the press-formed 45Ti–45Ni–10Nb alloy described in Sec. 3 showed that the alloy can be used for manufacturing the working element of the fire-protection device that we develop.

## CONCLUSIONS

(1) Our study has shown that the best thermomechanical characteristics of the 45Ti–45Ni–10Nb (at %) alloy samples can be achieved by deforming the samples in the range 11–15% at temperatures of –60...–70°C and a deformation rate of $1.2 \times 10^{-3}$ s$^{-1}$. These deformation conditions can provide an optimum combination of the shape memory characteristics ($\varepsilon_{SME} = 4.4$–$5.7\%$, $\eta_{SME} = 0.5$–$0.53$) and the temperatures of the shape recovery onset ($A^b_{s\,SME} = 23$–$42$°C, $A_{s\,SME} = 65$–$74$°C).

(2) We used the results of the study to develop a fire-protection device for nuclear power facilities.

## REFERENCES

1. D. B. Chernov, *Application of Shape-Memory Alloys in Engineering Constructions*, Ed. by A. V. Mitin (NIISU, Moscow, 1999) [in Russian].
2. N. N. Popov, *Designing Advanced Technologies Based on Shape-Memory Materials* (RFYaTs–VNIIEF, Sarov, 2008) [in Russian].
3. Yu. K. Kovneristyi, O. K. Belousov, S. G. Fedotov, N. M. Matveeva, and A. A. Klopotov, "Thermodynamic and structural aspects of the investigation of

alloys based on NiTi with a shape-memory effect," in *Titanium Alloys with Special Properties* (Nauka, Moscow, 1982) [in Russian].

4. V. A. Likhachev and S. R. Shimanskii, *Effect of the composition of the Ti–Ni–Nb alloy on its properties and workability,* Available from VINITY, No. 7865-84.
5. V. A. Udovenko, P. L. Potapov, S. D. Prokoshkin, I. Yu. Khmelevskaya, V. Ya. Abramov, and Yu. V. Blinov, "Study of functional properties of the Ti–45% Ni–10% Nb alloy with a wide hysteresis of the magnetic transformation," Metalloved. Term. Obrab. Met., No. 9, 19–22 (2000).
6. V. Ya. Abramov, N. M. Aleksandrova, D. V. Borovkov, S. Yu. Makushev, N. A. Polyakov, N. N. Popov, S. D. Prokoshkin, and I. Yu. Khmelevskaya, " Structure and functional properties of heat- and thermomechanically treated Ti–Ni–Nb-based alloys with a wide martensitic hysteresis. I. Ti–Ni–Nb ternary alloys, Phys. Met. Metallogr. **101**, 404–414 (2006).
7. N. N. Popov, V. F. Lar'kin, D. V. Presnyakov, A. A. Aushev, T. I. Sysoeva, A. A. Kostyleva, and E. B. Suvorova, "Investigation of thermomechanical characteristics of shape-memory alloys of the Ti–Ni–Nb system and of the effect of heat treatment on them," Phys. Met. Metallogr. **114**, 348–357 (2013).
8. N. N. Popov, V. F. Lar'kin, D. V. Presnyakov, and A. A. Kostyleva, "Investigation of mechanical characteristics of shape-memory alloys of the Ti–Ni–Nb system and of the effect of heat treatment on them," Zavod. Lab.: Diagn. Mater. **80** (8), 22–30 (2014).
9. N. N. Popov, T. I. Sysoeva, A. A. Aushev, V. F. Lar'kin, and A. A. Kostyleva, "Properties of a 45Ti–45Ni–10Nb shape memory alloy in the as-cast and pressed states," Russian Metallurgy (Metally) **2016** (11), 1055–1063.
10. N. N. Popov, T. I. Sysoeva, and E. N. Grishin, "Effect of heat-treatment conditions on the structure and phase transformations in the shape-memory 45Ti–45Ni–10Nb alloy in as-cast and press-formed states," Phys. Met. Metallogr. **118**, 292–303 (2017).
11. L. C. Zhao, "Study of Ti–Ni–Nb shape memory alloys with a wide hysteresis," Proc. Int. Symp. Shape Memory Materials, Kanazawa, Japan, May, 1999, Mater. Sci. Forum **327–328**, 23–30 (2000).
12. X. M. He and L. J. Rong, "DSC analysis of reverse martensitic transformation in deformed Ti–Ni–Nb shape memory alloy," Scr. Mater. **51**, 7–11 (2004).
13. N. N. Popov, A. I. Korshunov, A. A. Aushev, M. Yu. Sidorkin, T. I. Sysoeva, I. V. Kostylev, A. E. Gusarov, and V. V. Stolyarov, "Effect of nanostructurizing and rate of inducing deformation on the structural and thermomechanical characteristics of a titanium nickelide-based alloy," Phys. Met. Metallogr. **102**, 432–438 (2006).
14. N. N. Popov, RF Patent No. 2478928 (2011).
15. *Shape Memory Alloys: Fundamentals, Modeling and Applications*, Ed. by V. Brailovski, S. Prokoshkin, P. Terriault, F. Trochu (ETS Publ., Monreal, 2003).
16. Titanium Nickelide Shape-Memory Alloys, Ed. by V. G. Pushin (Uro RAN, Ekaterinburg, 2006) [in Russian].
17. V. E. Gyunter, V. N. Khodorenko, Yu. F. Yasenchuk, T. L. Chekalkin, V. V. Ovcharenko, A. A. Klopotov, G. Ts. Dambaev, P. G. Sysolyatin, N. G. Fomichev, V. N. Olesova, M. Z. Mirgazizov, A. V. Proskurin, R. V. Zigan'shin, V. K. Polenichkin, A. N. Matyunin, M. Yu. Fatyushin, N. A. Molchanov, and A. N. Monogenov, *Titanium Nickelide. New-Generation Medical Material* (Izd-vo MITs, Tomsk, 2006) [in Russian].
18. A. P. Kulaichev, *Universal Program Statistical Packet STADIA (version 7.0) for Windows* (NPO "Informatika i komp'yutery," Moscow, 2007) [in Russian].
19. A. P. Kulaichev, *Methods and Tools for a Complex Analysis of Data* (Forum: Infra-M, Moscow, 2006) [in Russian].
20. M. N. Stepnov, *Statistical Methods of processing of Data of Mechanical Tests* (Mashinostroenie, Moscow, 1985) [in Russian].

*Translated by T. Gapontseva*